OPTIMIZATION OF TWO LINEAR MODELS FOR ESTIMATING BRAIN DEFORMATION DURING SURGERY USING FINITE ELEMENT METHOD

Hajar Hamidian[1], Hamid Soltanian-Zadeh[1, 2], Reza Faraji-Dana[3], Masoumeh Gity[4]

[1] Control and Intelligent Processing Center of Excellence (CIPCE), School of Electrical and Computer Engineering, University of Tehran, Tehran, Iran.
E-mails: h.hamidian@ece.ut.ac.ir, hszadeh@ut.ac.ir
[2]Radiology Image Analysis Lab., Henry Ford Hospital, Detroit, MI 48202, USA
E-mail: hamids@rad.hfh.edu
[3] School of Electrical and Computer Engineering, University of Tehran, Tehran, Iran.
E-mail: reza@ut.ac.ir
[4]Department of Radiology, University of Tehran Medical School, Tehran, Iran.
E-mail: p_gity@yahoo.com

ABSTRACT

This paper optimizes two linear models implemented using finite element method for estimating brain deformation during craniotomy. These are mechanical models called solid-mechanic and elastic. Both models assume finite deformation of the brain after opening the skull. We use MRIs of different patients undergoing brain tumor surgery in two states of pre-operative and intra-operative. Anatomical landmarks in both images are specified by an expert radiologist. Tetrahedral mesh and function optimization are used to find the optimal modes by minimizing the mean distance between the actual and predicted locations of the anatomical landmarks. Based on the final value of the objective function, we conclude that the accuracy of the solid mechanic model is higher than that of the elastic model. This method estimates brain deformation using anatomical landmarks specified by an expert on pre-operative MRI without requiring intra-operative images.

1. INTRODUCTION

Mechanical property of very soft tissue such as brain, has been studied in recent years for applications like surgical planning [1]. However, in a common neurosurgical procedure, the brain deforms after opening the skull, causing misalignment of the subject to the preoperative images [2], [3]. This happens because of cerebrospinal fluid (CSF) leakage, dura opening, anaesthetics and osmotic agents, as well as conditions, which are different from the normal state [4], [5]. While the intraoperative imaging such as iMRI is the best way to determine this deformation, intraoperative images suffer from the constraints of the operating room [6]. This problem can be avoided by using biomedical models.

In this paper, two models are used as described next. The first model is based on the biphasic soft-tissue [7] that assumes the brain tissue behaves as a linear elastic material and indicates that the stress can be related to strain by Hook's law [8], [9]. The second model is based on the principle that the sum of the virtual work from the internal strains is equal to the work from the external loads [10], [11]. In most practical cases, such models utilize the finite element methods [12] to solve sets of partial differential equations governing the deformation behavior of the tissue. For solving these models, we must know the value of the brain's parameters. Previous works used approximate values of the brain parameters, which we also use in this work as initial values. We apply function optimization to optimize these parameters and minimize the distance between the predicted locations of the anatomical landmarks using the pre-operative images and their actual locations on the intra-operative images. We then compare the two models using their resulting errors.

In the next section, we explain two models and our method for solving these models using finite element methods and optimizing their parameters. In Section 3, we explain the results of our implementation on five cases of the brain and compare the models. Section 4 presents the conclusions of our work.

2. MATERIALS AND METHODS

Patient-specific geometric data are obtained from a set of five pre-operative and intra-operative MRI of patients undergoing brain tumor surgery. In order to specify the displacements of the brain tissue, anatomical landmarks are defined in both of the pre- and intra-operative images

Table I. Parameter used in equation (3)

Parameter symbol	Value
E	2100 Pa
υ	0.46
ρ_t	1000 kg/m^3
ρ_f	1000 kg/m^3
K	1e-7m^{3}s/kg
α	1
1/S	0
Ψ	0.001 Pa/s
G	E/2(υ +1) Pa

that are registered rigidly using the ITK software. The displacement of the landmarks can be defined by medical experts, imaging device such as MRI, CT, laser devices, or spectroscopic camera. As mentioned previously, the resolution of the intra-operative tomography images is low and thus it may be superior to image the exposed surface of the brain or tissues that are important for surgery like the tumor.

In order to distinguish between the brain parenchyma and tumor, the images are segmented using the 3D-Slicer. After the segmentation, three-dimensional models of the surfaces of the brain parenchyma and tumor are created using the COMSOL3.3. For creating the 3D model, the slices that are near the craniotomy surfaces, have higher resolutions than the slices far from the surface. After creating the 3D models, automatic 4-noded tetrahedral meshes with Lagrange shape functions are generated for both of the parenchyma and the tumor using the COMSOL3.3 software. An example of the mesh generated by the software is shown in Figure 1, which consists of 15,164 tetrahedral elements.

2.1. Biomedical Models

As mentioned in Section 1, for determining the deformation of the brain, a model of the brain may be used. Such a model provides numerical formulations that describe the behavior of the brain tissue. These formulations can be linear or non-linear [13], [14]. In this paper, we use and compare two models that describe the tissue behavior linearly.

In the first model (linear solid-mechanic model), the body is assumed to be a linear elastic continuum with no initial stresses or strains. The energy of the body's deformation caused by externally applied forces can be expressed as equation (1) [10].

$$E = \frac{1}{2}\int_{\Omega} \sigma^T \varepsilon \, d\Omega + \int_{\Omega} F^T u d\Omega, \qquad \varepsilon = \left(\frac{\partial u}{\partial x}, \frac{\partial u}{\partial y}, \frac{\partial u}{\partial z}, \frac{\partial u}{\partial x}+\frac{\partial u}{\partial y}, \frac{\partial u}{\partial y}+\frac{\partial u}{\partial z}, \frac{\partial u}{\partial x}+\frac{\partial u}{\partial z}\right)^T = Lu \tag{1}$$

Where σ is the stress vector and in the case of linear elasticity, with no initial stresses or strains, relates to the strain vector (ε) by the linear equation $\sigma = D\varepsilon$. The description of the parameters can be found in [10]. The value of D depends on two material parameters: the

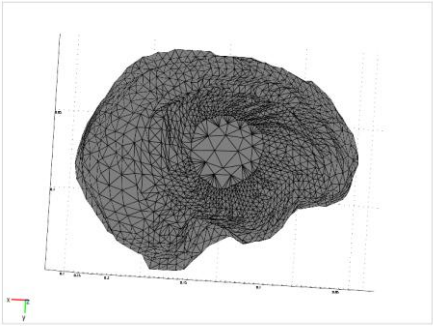

Figure 1. The result of meshing a brain volume.

Young modules and the Poisson ratios. According to [10]-[11], the solution to these equations can be written in a global linear equation (2).

$$Ku = -F \tag{2}$$

We rely on the study of Ferrant *et al* in [10] and choose our initial coefficients (Young modules = 3 kPa, Poisson ratio = 0.45).

The second model (linear elastic model), assumes that the deformation of the brain tissue as a poroelastic material occurs because of its elastic behavior and the pressure of exteracellular fluid. Based on these assumptions, the model can be written as equation (3) [15], [16].

$$\nabla.G\nabla u + \nabla\frac{G}{1-2\upsilon}(\nabla.u) - \alpha\nabla p = (\rho_t - \rho_f)g$$
$$\alpha\frac{\partial}{\partial t}(\nabla.u) - \nabla.k\nabla p + \frac{1}{S}\frac{\partial p}{\partial t} = \Psi \tag{3}$$

The description of parameters can be found in [4]. The initial value of parameters can be seen in Table I.

Generally, the brain can be supposed as a saturated material thus omitting the derivation of the pressure with respect to time in equation (3) (i.e., $\alpha = 1, 1/S = 0$). This model allows accessing more elastic boundary conditions of the intracranial pressure by modeling CSF drainage while maintaining linearity. That is an important computational advantage.

2.2. Boundary Conditions

For solving we need boundary conditions to solve the equations. In both models, we assume the exposed surface is free to move and the remaining surface is fixed. For the first model, we have conditions for the displacement variable and force per unit (F). We use $F=u$ for the boundary conditions of the fixed boundary nodes because the elements of the rigidity matrix K in equation (2) for which the deformation is supposed to be known need to be set to zero and the diagonal elements to one. More details can be found in [10]. For the exposed surface, we assume its nodes are free to change. The initial value of the parameter F is set by examining the MR images of five different patients. The exact value of F for each part is determined by the optimization process. For the second model, the boundary condition for pressure (p) instead of

the displacement variable is needed. The corresponding nodes in the mesh lying above the level of intra-operative CSF drainage are assumed to reside at the atmospheric pressure (Dirichlet condition in pressure), while those that do not, are the non-draining regions of the brain (Neumann condition in pressure).

2.3. Optimization Process

The parameters of the brain in each model are not the same for different patients and thus usually approximated parameters are used. In this paper, we use an optimization process to optimize these parameters and achieve most accurate results with respect to the real deformations. To this end, we choose a cost function defined as the sum of the distances between the actual positions of the anatomical landmarks in the intra-operative images and their estimated positions based on the deformations of the pre-operative images by the two models. We use the Maltlab optimization toolbox to optimize the cost function and find the optimal values of the parameters as explained next.

In the first model, we do not know the exact value of the force applied to the center of the exposed surface of the brain. This parameter is found by the optimization process. In addition, the two parameters (Young modulus and Poisson's ratio) reported in the literature are not the same for different patients and thus they will be also optimized.

For the second model, the parameters in Table I except for $\alpha, 1/S$ are optimized. This is because, as mentioned in Section 2.1, we model the brain as a saturated material for which the derivative of the pressure with respect to time is omitted in equation (3) (i.e., $\alpha = 1, 1/S = 0$). We determine the brain's deformation in the steady state, meaning that we do not consider the transient changing of p in equation (3) and thus Ψ / k is optimized.

3. RESULTS

For estimating the deformation of the brain, we use a set of five pre-operative MRIs of different patients undergoing brain tumor surgery. These data were taken in two states of pre-operative and intra-operative. The intra and pre-operative images are registered rigidly, and then special points are determined by expert physiologist in both pre- and intra-operative images. In this paper, approximately 60 points are selected by physiologist in each data. The half points are used in optimization process and the other half are used to test the method. As mentioned before, the brain and the tumor are segmented using 3D SLICER and 3D model of brain and tumor are created using COMSOL3.3. For meshing and solving process we use COMSOL3.3 and for optimization process, we use MATLAB optimization toolbox. The results of both models can be found in Figures 2-3. As it can be seen in both model the estimated tumor in 2D and 3D have a good matching with real intra-operative tumor and the accuracy of both model for tumor are acceptable but the accuracy of fist model is better. This can be seen in larger scale better. The tolerance of parameters can be seen in Table II and the mean and maximum of displacement error can be seen in Table III. As can be seen from Table III, For special points which are specified by physiologist that are mostly near the exposed surface, the accuracy of both models are acceptable but first model is better. This method can be used for estimation the deformation of the exposed brain without using intra-operative images.

4. CONCLUSION

In estimating the brain deformations, model selection is an important step for obtaining accurate and reliable results. To this end, we studied two linear mechanical models for describing the mechanical properties of the brain based on finite deformation and optimization of their parameters for a simple sphere and real models of the brain extracted from MRI. The first model is based on the virtual works, applied to the inside and outside of the brain, but the second model is based on the equations that relate the displacement of the volume to the pressure of the fluid. Results of our method in both modeling and matching the estimated and intra-operative tumor in two and three dimensions are good but the points near exposed surfaces have a better matching in the first model. These results confirm that we can estimate the deformation of the brain without using the intra-operative images.

5. ACKNOWLEGEMENTS

Patient-specific geometric data for the brain were obtained from a set of pre- and intra-operative MRIs of three different patients undergoing brain tumor surgery at the Surgical Planning Laboratory, Brigham and Women's Hospital (Harvard Medical School, Boston, Massachusetts, USA). The authors gratefully acknowledge Dr. Ron Kikinis and Dr. Tina Kapur for providing this data.

REFERENCES

[1] A. Wittek, K. Miller, J. Laporte, R. Kikinis, S. Warfield, "Computing reaction forces on surgical tools for robotic neurosurgery and surgical simulation," *CD Proceedings of Australasian Conference on Robotics and Automation ACRA. Canberra*, Australia, 2004.

[2] K. Miller, "Method of testing very soft biological tissues in compression," *J. Biomechanics*, vol. 38, pp.153–158, 2005.
[3] M. I. Miga, K. D. Paulsen, P. J. Hoopes, F. E. Kennedy, J. A. Hartov, and D. W. Roberts, "In Vivo quantification of a homogeneous brain deformation model for updating preoperative images during surgery," *IEEE Trans. Biomed. Eng*., vol. 47, no. 2, pp. 266-273, Feb. 2000.
[4] P. Dumpuri, R. C. Thompson, B. M. Dawant, A. Cao, M. I. Miga, "An atlas-based method to compensate for brain shift: Preliminary results," *Medical Image Analysis*, vol. 11, pp. 128–145, 2007.
[5] L. A. Platenik, M. I. Miga, D. W. Roberts, K. E. Lunn, F. E. Kennedy, A. Hartov, and K. D. Paulsen, "In vivo quantification of retraction deformation modeling for updated image-guidance during neurosurgery," *IEEE Trans. Biomed. Eng*., vol. 49, no. 8, pp. 823-835, Aug. 2002.
[6] Clatz, H. Delingette, I. F. Talos, A. J. Golby, R. Kikinis, F. A. Jolesz, N. Ayache, and S. K. Warfield, "Robust nonrigid registration to capture brain shift from intraoperative MRI," *IEEE Trans. Med. Imag.*, vol. 24, no. 11, pp. 1417-1427, Nov. 2005.
[7] K. D. Paulsen, M. I. Miga, F. E. Kennedy, P. J. Hoopes, A. Hartov, and D. W. Roberts, "A computational model for tracking subsurface tissue deformation during stereotactic neurosurgery," *IEEE Trans. Biomed. Eng*., vol. 46, no. 2, Feb. 1999.
[8] K. D. Paulsen, M. I. Miga, D. W. Roberts, F. E. Kennedy, L. A. Platenik, K. E. Lunn, and A. Hartov, "Finite element modeling of tissue retraction and resection for preoperative neuroimage compension with surgery," *Medical Imaging 2001: Visualization, Display, and Image-guided Procedures*, vol. 2, no. 24, pp. 13-21, 2001.
[9] M. I. Miga, T. K. Sinha, D. M. Cash, R. L. Galloway, and R. J. Weil, "Cortical surface registration for image-guided neurosurgery using laser-range scanning," *IEEE Trans. Med. Imag.*, vol. 22, no. 8, pp. 973–985, Aug. 2003.
[10] M. Ferrant, A. Nabavi, B. Macq, P. M. Black, F. A. Jolesz , R. Kikinis, and S. K. Warfield, "Serial registration of intraoperative MR images of the brain," *Med. Imag. Analysis*, vol. 6, p.p. 337–359, 2002.
[11] M. Ferrant, A. Nabavi, B. Macq, F. A. Jolesz, R. Kikinis, S. K. Warfield, "Registration of 3-D intraoperative MR images of the brain using a finite element biomechanical model," *IEEE Trans. Med. Imag.*, vol. 20, pp.1384–1397, 2001.
[12] K. J. Bathe, "Finite element procedures," *Prentice-Hall*, Englewood Cliffs, NJ. 1996.
[13] Wittek, K. Miller, R. Kikinis, S. K. Warfield, "Patient-specific model of brain deformation: Application to medical image registration," *J. Biomech.*, in press, Accepted 27 February 2006.
[14] A. Wittek, R. Kikinis, S. K. Warfield, and K. Miller, "Computation using a fully nonlinear biomechanical model," *in proc. of MICCAI 2005, LNCS, Springer-Verlag, Berlin Heidelberg*, vol. 3750, pp. 583 – 590, 2005.
[15] M. I. Miga, K. D. Paulsen, J. M. Lemery, S. D. Eisner, A. Hartov, F. E. Kennedy, and D. W**.** Roberts, "Model-Updated Image Guidance: Initial clinical experiences with gravity-induced brain deformation," *IEEE Tran. Med. Imag***.,** vol. 18, no. 10, Oct. 1999.
[16] K. E. Lunn, K. D. Paulsen, F. Liu, F. E. Kennedy, A. Hartov, and D. W. Roberts, "Data-guided brain deformation modeling: evaluation of a 3-D adjoint inversion method in porcine studies," *IEEE Trans. Biomed. Eng*., vol. 53, no. 10, pp. 1893-1900, Oct. 2006.

TABLE II- Initial and estimated parameters for the first and second model.

	Optimized in five cases	Model
Young modulus	0.45 ± 0.029657	1st model
Poisson's ratio	3000 ± 269.399	1st model
Resultant Force	222.4 ± 54.95614	1st model
E	2100± 204.9833	2nd model
ν	0.45 ± 0.021409	2nd model
ρ_t	1000 ± 40.5628	2nd model
ρ_f	1000 ± 12.8952	2nd model
Ψ /k	1.01e4 ± 032.1643	2nd model

TABLE III-Maximum and mean error of displacement between estimated point and real point

Maximum error for 1st model	$\Delta x = 3.35 \pm 0.65mm$ $\Delta y = 3.6 \pm 0.8mm$ $\Delta z = 0.5955 \pm 0.2465mm$
Maximum error for 2nd model	$\Delta x = 3.42 \pm 0.42mm$ $\Delta y = 3.615 \pm 0.785mm$ $\Delta z = 0.7445 \pm 0.3005mm$
Mean error for 1st model	$\Delta x = 1.255 \pm 0.385mm$ $\Delta y = 1.275 \pm 0.425mm$ $\Delta z = 0.348 \pm 0.215mm$
Mean error for 2nd model	$\Delta x = 1.31 \pm 0.24mm$ $\Delta y = 1.345 \pm 0.455mm$ $\Delta z = 0.414 \pm 0.22mm$

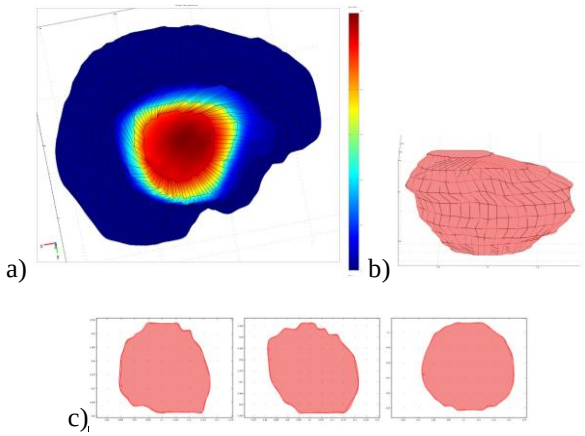

Figure 2. Result of the second model, a) 3D result of brain deformation, b) 3D comparison of tumor deformation c) 2D result for tumor

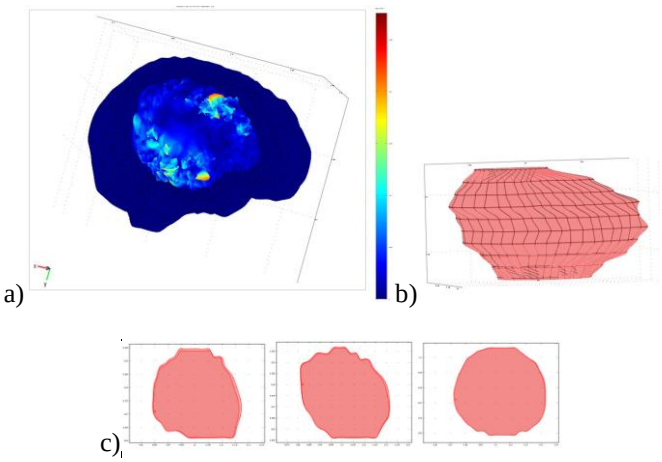

Figure 3. Result of the second model, a) 3D result of brain deformation, b) 3D comparison of tumor deformation c) 2D result for tumor